Thermodynamics of the Lithium Loop in a Liquid Metal Divertor for Future Fusion Reactors

R. Zanino[1], D. Aquaro[2], S. Carli[1], G. Caruso[3], F. Crisanti[4], A. Facchini[2], R. Lo Frano[2], G. Mazzitelli[4], G. F. Nallo[1], L. Savoldi[1], F. Subba[1], G. Vella[5]

[1]NEMO group, Dipartimento Energia, Politecnico di Torino, Torino, Italy

[2]Università di Pisa, Pisa, Italy

[3]Università degli Studi di Roma "La Sapienza", Roma, Italy

[4]ENEA Frascati, Italy

[5]Università degli Studi di Palermo, Palermo, Italy

E-mail contact of main author: roberto.zanino@polito.it

Abstract. Solutions for the steady-state power exhaust problem in future fusion reactors (e.g. DEMO) are not automatically provided by present experiments or even ITER, because the expected heat fluxes, as well as the level of neutron irradiation, will be much higher. Dedicated work packages are being devoted to this problem within EUROfusion and even a dedicated facility (the Divertor Tokamak Test – DTT) is being proposed by Italy. Among the possible solutions, a liquid metal (LM) divertor has been proposed more than 20 years ago. The particularly attractive feature of this solution is obviously the absence of damage to the wall, even in case of large heat fluxes, thanks to the high latent heat of evaporation, to the liquid nature of the wall –that can be refilled- and to the lithium vapor shield effect. The present work aims at developing a first model of the LM loop, which will be the core of the tools to be developed and eventually applied to the conceptual design of an LM divertor for the DTT facility. The model will describe the transport of the LM in the evaporation chamber, including its interaction with the plasma.

1. Introduction and background

Safe power exhaust, even in steady state, is one of the major issues in fusion reactors and a potential show-stopper towards the production of the first kWh from the fusion energy source, which the EU roadmap [1] has set at the target for its DEMO reactor in 2050. The power produced by deuterium-tritium reactions in the alpha particles channel may be partly, more or less isotropically radiated, but the rest reaches the plasma-facing components (PFCs) in the strongly anisotropic channel of plasma advection-conduction. This leads to high particle and heat fluxes, because of the relatively small wetted areas associated to the scrape-off layer (SOL) predicted in future machines, affecting not only the PFCs lifetime but also the core plasma purity (measured by the Z_{eff} parameter).

In ITER the control of the steady-state peak heat load (q_{peak} below 10 MW/m^2) on the PFCs and on the Z_{eff} relies on a single-null divertor with solid (W) target and on the Be first wall (FW), combined with detached plasma operation and seed impurity puffing [2], [3]. Even if this complex combination of conditions should be confirmed experimentally in ITER, extrapolation to DEMO is not automatically guaranteed. Furthermore, as the increase in size from ITER to DEMO is much less than the increase in the design thermal power to be produced by the two machines, in DEMO it will be even more difficult to meet the technological constraints on q_{peak} related to the use of a solid divertor.

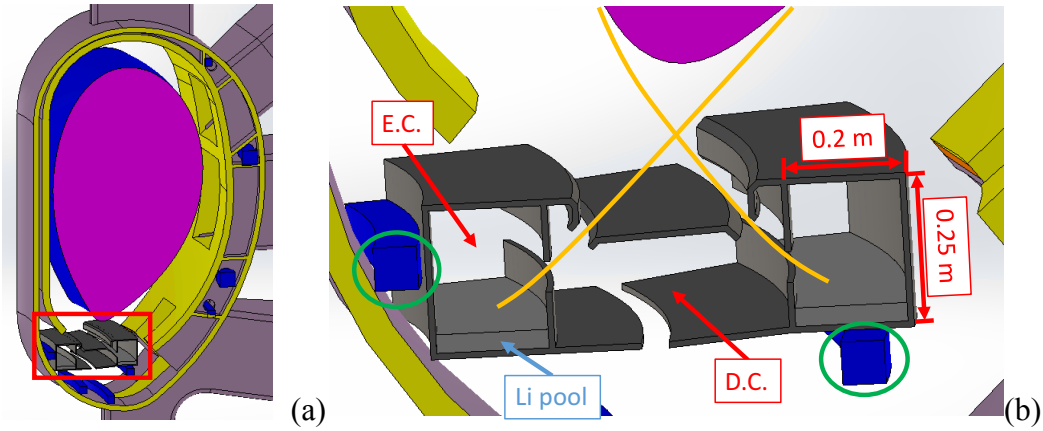

FIG. 1: DTT main plasma chamber with the divertor highlighted (a) and a zoom of the preliminary sketch of the liquid metal divertor (b)

The risk-mitigation strategy currently foresees two radically different approaches, of which the one especially relevant for our work here is the LM divertor. Indeed, the LM evaporation could in principle guarantee the exhaust of hundreds (!) of MW/m^2, as far as the effects of this evaporation on the plasma are not taken into account, with much more limited, if any, damage to the target than the solid target option, and consequent increase of the divertor lifetime.

Possible LM choices include in the first place Li, which will be considered here, but also others, e.g. Sn. As to the LM target, different options are being considered, ranging in complexity from a simple pool to a thin liquid film, to the use of the so-called capillary porous structure (CPS) [4], recently tested on the liquid Li limiter (LLL) in FTU [5]. While the CPS should guarantee, better than other solutions, the avoidance of splashing phenomena with generation of LM droplets, which could easily compromise the plasma purity, we will refer in the present work to the simpler case of a LM pool without CPS and without external (pumped) circulation of the LM. In the EU, significant attention is being given to these problems within the EUROfusion Work Packages DTT1 and DTT2, where DTT stays for Divertor Tokamak Test, an Italian proposal for a machine entirely devoted to the issues of power exhaust and Z_{eff} in DEMO perspective [6]. The EU is considering to test LM-based modules in existing medium-size tokamaks (e.g., ASDEX Upgrade) [7], and Italy is proposing to build the DTT facility and host it at the ENEA laboratories in Frascati.

2. System description

Starting from the drawing of the DTT chamber, a first preliminary sketch of a possible liquid metal divertor geometry to fit in the available space has been prepared, see FIG. 1. This is based on the idea originally proposed by Nagayama [8]: the SOL plasma flowing towards a liquid Li

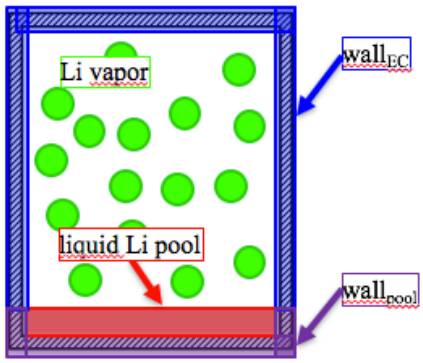

FIG. 2. Schematic representation of the computational domain

pool enters, after the main plasma chamber, first the Differential Chamber (DC, see FIG. 1) and finally the Evaporation Chamber (EC), where the pool is located. The relative position of the openings is more or less compatible with a reference Single Null (SN) DTT equilibrium.

In this preprint, due to lack of space, only the model of the EC will be presented. For the sake of simplicity, the system is assumed to be closed but not isolated, since the heat load and particle loads associated with the plasma are allowed to enter, and the walls are considered to be actively cooled.

The schematic representation of the EC used to write down the model equations is shown in FIG. 2. Its relevant sub-systems are:

- the liquid Li in the pool;
- the Li vapor in the remaining volume of the chamber;
- the solid walls in contact with the liquid Li (identified in the following with subscript *pool*);
- the solid walls in contact with the Li vapor (identified in the following with subscript *EC*).

The boundary of the Li vapor region will be subdivided into pool surface and $wall_1$.

3. Relevant physical phenomena in the EC

3.1 Evaporation/condensation from/to the pool

The net evaporation/condensation rates from the surfaces in contact with the Li vapor have been evaluated by means of the Hertz-Knudsen equation [9].

While this expression is likely to be appropriate for describing the Li evaporation/condensation fluxes from/to the pool, it has to be considered only as a very first approximation for the Li evaporation/condensation fluxes from/to the walls, due to the strong effect of the wall temperature on the interface. It should be remarked that the walls of the EC are assumed to be coated by lithium (either a liquid Li film -in the Nagayama proposal- or a liquid Li-filled wick -in case a CPS is employed-).

3.2 Sputtering from the pool

The adopted formulation for the erosion flux of Li from the pool under D plasma bombardment is reported in [10]. It allows to evaluate the flux of sputtered Li emitted from a liquid Li surface subjected to plasma bombardment as a function of the surface temperature, the plasma conditions at the target -in terms of ion temperature and density- and the concentration of hydrogenic species (retention) in the liquid layer. The latter is in particular responsible of a strong reduction of both the evaporation and the sputtering mass fluxes.

However, for the sake of simplicity, we will assume hereafter no D retention in the Li pool.

3.3 Interaction of the Li vapor with the SOL plasma: the Li “vapor shield”

Experimental results (see [11], [12]) suggest that the capability of Li of reducing the target heat load is not only associated to its latent heat of vaporization. Indeed, the power and particle fluxes on the pool surface are reduced by this “vapor shield” (and therefore also the evaporation/sputtering sources), provided one includes the cooling of the plasma by ionization and line/bremsstrahlung radiation [13] of the Li vapor shield in front of the target, which could lead to a more easily manageable flux of Li vapor transported towards the core plasma.

For the time being, a simplified approach is used: the amount of the incoming heat load associated with the plasma, which is radiated by the Li vapor shield, is evaluated as [14]

$$\Phi_{rad} = E_{rad,pot,z} \cdot e \cdot \dot{N} \quad (1)$$

where $E_{rad,pot,z}$ is the total energy radiated by a single impurity (i.e. Li) particle during its lifetime in the plasma in eV, e is the conversion factor from eV to J and $\dot{N}$ is the total impurity influx in particles/s (which in the following will be considered equal to the evaporated Li mass flux). The radiated energy is then subtracted from the plasma heat load. The radiated power is partly directed towards the pool surface and partly directed towards the walls, and it is assumed to be completely absorbed by walls/pool surface.

4. Model description

4.1 Assumptions:

1. Li vapor is approximated as an ideal gas due to the very low pressure foreseen in the EC –below 10^{-2} Pa- as compared to the critical pressure of Li, which is ~800 bar [15];
2. Li vapor is monoatomic (the fraction of Li_2 in vapor phase is between 5 and 10% at the temperatures foreseen for this system [15]);
3. Toroidal symmetry: the problem is reduced from 3D to 2D;
4. Uniform temperature and density on the 2D cross section of each of the control volumes presented in FIG. 3: the system is reduced from 2D to a set of coupled 0D sub-systems;
5. The Li vapor is optically thin with respect to radiation;
6. The Li pool is optically thick, i.e. it absorbs all radiated power directed towards it;
7. The Li liquid and vapor temperatures are assumed equal ($T_{vap} = T_{pool}$);
8. Condensed lithium on the walls is instantaneously returned to the pool, without convective heat transfer between Li film and the walls;
9. Radiation from the liquid Li pool surface to the (colder) walls is checked a posteriori to be negligible with respect to radiation from the Li vapor shield.

4.2 Simplified 0D model

In this first part of the analysis a simplified 0D model has been derived and implemented.

Due to the nonlinear nature of the problem, the transient terms in the equations have been retained, which makes it easier to numerically solve them, but the interest is in the steady state values of temperatures and density within the system.

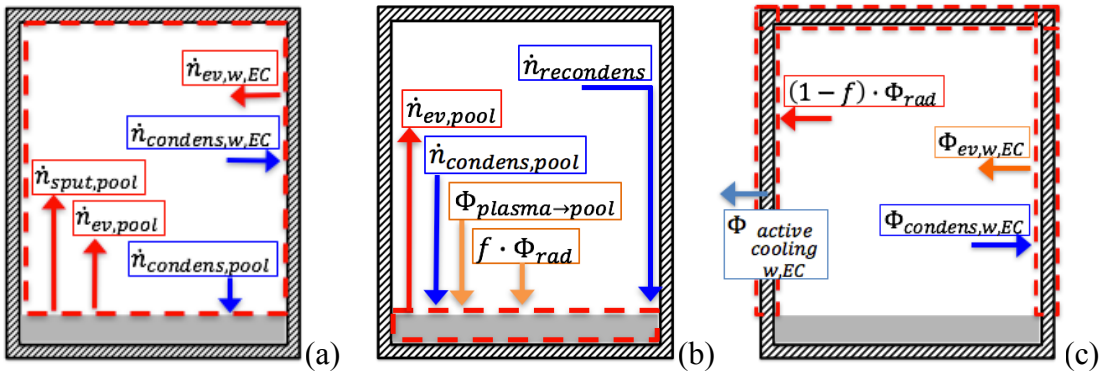

FIG. 3. Control volumes for mass conservation in the vapor phase (a), for mass and energy conservation in the pool (b) and for the walls power balance (c).

1. Conservation of mass for the Li vapor (control volume shown in FIG. 3(a)):

$$\frac{dN_{vap}}{dt} = \left(\dot{N}_{ev,w,EC} - \dot{N}_{condens,w,EC}\right) + \left(\dot{N}_{ev,pool} - \dot{N}_{condens,pool}\right) + \dot{N}_{sput,pool} \quad (2)$$

where

- N_{vap} is the number of Li atoms present in the vapor phase;
- $\dot{N}_{ev,w,EC}$ is the gross (as opposed to net) evaporation rate from the walls in atoms/s;
- $\dot{N}_{ev,pool}$ is the gross evaporation rate from the liquid-vapor interface in atoms/s;
- $\dot{N}_{condens,w,EC}$ is the gross condensation rate to the walls in atoms/s;
- $\dot{N}_{condens,pool}$ is the gross condensation rate to the liquid-vapor interface in atoms/s;
- $\dot{N}_{sput,pool}$ is the sputtering rate from the liquid-vapor interface in atoms/s.

2. Conservation of mass for the liquid Li layer (control volume shown in FIG. 3(b)):

$$\frac{dN_{pool}}{dt} = -\dot{N}_{ev,pool} + \dot{N}_{condens,pool} + \dot{N}_{recondens} \quad (3)$$

where

- N_{pool} is the number of Li atoms present in the liquid Li layer;
- $\dot{N}_{recondens}$ is the net condensation rate to the walls in atoms/s.

3. Energy conservation equation for the liquid Li layer (control volume shown in FIG. 3(b)):

$$\frac{dU_{pool}}{dt} = f \cdot \Phi_{rad} - (G \cdot h)_{ev,pool} + (G \cdot h)_{condens,pool} + \Phi_{plasma \to pool} + (G \cdot h)_{recondens} - \Phi_{pool \to w} \quad (4)$$

where:

- U_{pool} is the internal energy of the Li in the pool in J;
- $V_{pool}(t)$ is the volume of the liquid Li expressed in m^3;
- ρ_l is the density of the material used for the walls in kg/m^3;
- c_l is the specific heat of the material used for the walls in J/(kg·K);
- f is the fraction of Φ_{rad} which is irradiated towards the Li pool. The remaining fraction $(1-f)$ is directed towards the walls. As a first approximation, $f \approx \frac{A_{pool}}{A_{w,EC}+A_{pool}}$;
- $\Phi_{plasma \to pool}$ (W) is the amount of the incoming plasma heat load which is not radiated, evaluated as:

$$\Phi_{plasma \to pool} = \Phi_{SOL} - \Phi_{rad} \quad (5)$$

  where Φ_{SOL} is the incoming heat load associated with the plasma;

- $\Phi_{pool \to w}$ (W) is the power transferred from the liquid Li in the pool to the fraction of the wall in contact with it. In this simplified model the heat conduction between $wall_{EC}$ and $wall_{pool}$ is neglected. It is also assumed that the heat capacity of the fraction of the wall in contact with liquid Li is negligible. Hence the following identity holds:

$$\Phi_{pool \to w} = \Phi_{active\ cooling,w,pool} \quad (6)$$

  where $\Phi_{active\ cooling\ walls,pool} = H \cdot A_{w,pool} \cdot \left(T_{w,pool} - T_{water}\right)$. In the latter, H is the heat transfer coefficient between the wall and the cooling water in $W/(m^2K)$, $A_{w,pool}$ is the interface area in m^2 and T_{water} is the temperature of the cooling water;

- The $G \cdot h$ terms represent the heat fluxes associated to mass fluxes, evaluated as the product of the mass flow rates in kg/s and the specific enthalpies of Li in J/kg.

4. Energy conservation for the walls not in contact with liquid Li (control volume shown in FIG. 3(c)):

$$V_{w,EC} \cdot (\rho c)_{w,EC} \frac{dT_{w,EC}}{dt} = (1-f) \cdot \Phi_{rad} + (G \cdot h)_{condens,w,EC} - (G \cdot h)_{ev,w,EC} - \Phi_{active\ cooling,w,EC} \qquad (7)$$

where

- $V_{w,EC}$ is the volume of wall$_{EC}$ expressed in m^3;
- $\Phi_{active\ cooling,w,EC}$ is the power in W removed from the walls of the EC not in contact with the Li pool by means of active cooling, which can be preliminarily estimated as:

$$\Phi_{active\ cooling,w,EC} = H \cdot A_{w,EC} \cdot \left(T_{w,EC} - T_{water}\right) \qquad (8)$$

where $A_{w,EC}$ is the interface area in m^2.

5. Results

TABLE I summarizes the input data used for the calculations. The further assumption that $\dot{n}_{sput,pool} \approx 0$ has been made, which is reasonable for temperatures >500 °C provided the ion temperature is sufficiently low [10]. This requires a more detailed analysis. Notice also that $\Phi_{SOL} = 32$ MW corresponds in a 0D model like ours to a flux $\frac{\Phi_{SOL}}{A_{pool}} \sim 7$ MW/m^2 , whereas the estimated peak heat flux from 2D analysis [6] is ~ 55 MW/m^2. The walls are assumed to be made of stainless steel, and their thermophysical properties are consequently evaluated. The properties of liquid Li are according to [16].

The transient calculation starts from an equilibrium situation in which the water providing the active cooling is at a temperature slightly above the Li melting point (~180 °C), with the walls at the same temperature and a very small quantity of vapor, corresponding to the equilibrium value at that temperature.

At time $t = 0^+$ the heat load associated with the plasma is turned on. At the beginning, this heat load is almost entirely directed towards the pool, since the effect of the lithium vapor shield is small, due to the small evaporation fluxes, see eq. (1). This drives an initial steep temperature

TABLE I: INPUT DATA

Quantity	Value	Unit	Motivation for the choice
Φ_{SOL}	32	MW	Reference value for DTT [6]
A_{pool}	4.56	m^2	From the preliminary CAD
$A_{w,1}$	15.9	m^2	"
f	0.169	-	"
T_{water}	200	°C	Slightly higher than Li melting point [11]
H	5000	W/(m^2· K)	Reasonable value for water forced convective cooling
$E_{rad,pot,z}$	0-250	eV	Range adopted for the parametric study [13]

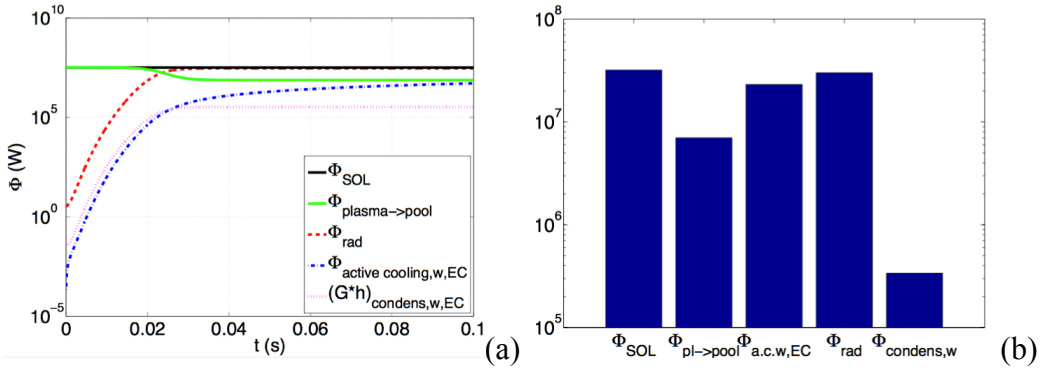

FIG. 4. Evolution of the power exchanged during the first part of the transient in the different channels (a) and corresponding steady state values (b)

increase of the Li system (vapor and liquid, assumed isothermal) and of the vapor density. The consequent increase of the evaporation rate from the pool causes the radiated fraction of the incoming heat load to increase. At this point the heat load to the pool has been reduced and the Li temperature reaches a steady state value determined by the balance between this power and $\Phi_{pool \rightarrow w}$. The steady state temperature of wall_{EC} is determined by the balance between the radiated power on the walls and $\Phi_{active\ cooling,w,1}$, since the heat flux associated to the condensing mass flow rate is negligible (see FIG. 4(a), where $E_{rad,pot,z} = 100\ eV$). The short time required to reach the steady state is in agreement with experimental results from Magnum-PSI facilities and FTU (see [10], [11]).

Since the correct value of $E_{rad,pot,z}$ is uncertain, a parametric study has been performed, whose results are shown in FIG. 5, starting from 0 up to 100 eV per particle. As this parameter is increased, the incoming heat load associated to the plasma is increasingly spread over the entire EC, instead of being only directed towards the Li pool. This implies a lower temperature of the liquid-vapor system (and therefore a lower vapor density) and a higher wall temperature.

6. Conclusions and future work

A first 0D model of a possible liquid Li divertor for the DTT machine has been developed and applied to a reference scenario. The results suggest the effectiveness in spreading the heat load associated with the plasma over a much larger surface area (in this case $A_{w,1}$). This could be achieved by means of the Li latent heat of evaporation alone, but the Li vapor shield effect greatly enhances this capability.

The key feature of this model is its modularity: additional (or improved) pieces of physics can be easily added in order to make it more comprehensive and/or accurate.

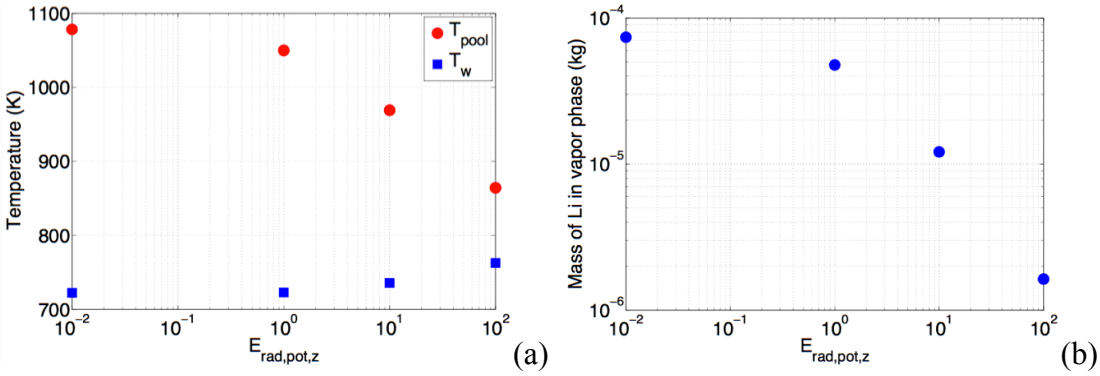

FIG. 5. Parametric study of the effects of the radiated energy per impurity particle: liquid and wall temperatures (a) and mass of vapor (b)

Although some correlations used still have room for improvement, the closure of the Li loop in the EC is almost achieved, the only missing piece being the flow of re-condensed liquid Li along the walls.

In the future, the model will be improved by including Li vapor efflux towards the DC, the differential pumping within the latter and the reduction of the efflux associated to the plasma entrainment effect. A more detailed description of the plasma cooling is also foreseen, in order to reduce the uncertainties associated to $E_{rad,pot,z}$. This can be achieved by means of simplified 0D models or by means of the SOLPS package.

Evolution of D concentration in the pool could also be evaluated in order to consider the evaporation suppression and to assess the D (and T) retention issues associated with this concept.

Acknowledgements

The authors would like to thank Giuseppe di Gironimo for the DTT CAD and Rob Goldston for discussions.

References

[1] ROMANELLI, F. et al., "Fusion electricity. A roadmap to the realisation of fusion energy" (2012).
[2] PITTS, R., "Physics basis and design of the ITER full-tungsten divertor", 55th Annual Meeting of APS Division of Plasma Physics, Denver (2013).
[3] MEROLA, M. et al, "Overview and status of ITER internal components", Fus. Eng. Des. **89** (2014).
[4] GOLUBCHIKOV, L. G. et al., "Development of a liquid-metal fusion reactor divertor with a capillary-pore system", J. Nucl. Mater. **233-237** (1996).
[5] MAZZITELLI, G. et al., "Heat loads on FTU liquid lithium limiter", Fus. Eng. Des. **86** (2011).
[6] ENEA, Divertor Tokamak Test Facility Project Proposal, Frascati (2015).
[7] DE BAAR, M. et al., Report of the STAC Ad Hoc Group on a strategy to address exhaust issues in the EU Fusion programme - Phase 1 (2013).
[8] NAGAYAMA, Y., "Liquid lithium divertor system for fusion reactor", Fus. Eng. Des. **84** (2009).
[9] SAFARIAN, J. and ENGH, T. A., "Vacuum Evaporation of Pure Metals", Metallurgical and Materials Transactions A, **44A** (2013) 747.
[10] ABRAMS, T., JAWORSKI, M. et al., "Suppressed gross erosion of high-temperature lithium via rapid deuterium implantation", Nucl. Fusion **56** (2016) 016022.
[11] MAZZITELLI, G., "Liquid metal: feedback from FTU", 22nd Int. Conference on Plasma Surface Interaction in Controlled Fusion Devices, Rome (2016).
[12] ONO, M., "Lithium As Plasma Facing Component for Magnetic Fusion Research," Princeton Plasma Physics Laboratory Report PPPL 4808 (2012).
[13] GOLDSTON, R. et al., "The lithium vapor box divertor", Phys. Scr. **T167** (2016).
[14] STANGEBY, P. C., The Plasma Boundary of Magnetic Fusion Devices, Institute of Physics Publishing, Toronto (2000).
[15] PASCAL, P., Nouveau traité de Chimie Minérale, Masson ed., Paris (1966).
[16] IAEA, Thermophysical Properties of Materials For Nuclear Engineering: A Tutorial and Collection of Data, Vienna (2008).